

INTRODUCTION

Numerous leading technologies are established in the aeronautical sector, wide spectrum of researches and developments are in progress in that areas ([1] and [2]) in which the propulsion systems of the aircrafts are also included [3]. Today, the application range of the gas turbine engines has increased significantly. This is especially true for the jet engines, which are the only applicable propelling systems of the high power commercial and military airplanes these days.

Moreover, the gas turbines are employed also in the other parts as oil, gas and energy production. In spite of the fact that those engines in comparison with piston ones don't have high thermal efficiency ("28 to 40%") they have substantial advantages in powerfulness, power density (power of the engine/mass of the engine), compactness, streamlining, simplicity and low maintenance cost demands. These engines are less sensitive for the overloads and they produce less vibration due to the well balanceable and rather axisymmetric rotational components. The gas turbines have high availability ("~97%") and reliability ("> 99%"), they have low emission (there is no lubricant in the combustion chamber and no soot during transient loads) they contain less moving parts and represent less sensitivity for the quality of the fuel compared to the piston engines. Additionally, there is no need for liquid-based cooling system, but the maximum allowable temperature ("~ 1500 C°") at the turbine inlet section must be limited due to the metallurgical reasons [4].

The small sized gas turbines are widely used for ground-based, vehicular applications, starter engine, APU (Auxiliary Power Unit) and research jet engine in academic applications due to low weight, easy to move and relative low cost. Furthermore, the utilization of this kind of engines has increased significantly as they are also applicable for remote-control airplanes or on unmanned aerial vehicles (UAVs) due to high thrust to weight ratio [5].

The small gas turbine includes power delivery under 5 MW. Typically, they are consisting of centrifugal compressor, combustion chamber and axial turbine. The centrifugal compressors have several advantages in compared with axial compressors especially for small gas turbines, at which the sizes are smaller and so the boundary layer thickness (δ) is relatively high. The centrifugal compressors are shorter, simpler and cheaper constructions and the blade numbers per stage is less than in case of axial compressors. The centrifugal compressors has higher pressure ratio per stage, they can resist better for surge and for impact of flying object. These types of compressors can fit to systems better with high pressure drop, because the outlet velocity is less. They have favourable isentropic efficiency below 5 kg/s mass flow rate, it is easier to balance, they are not much sensitive to the sudden variation of mass flow rate in time than the axial compressors. The operation and the maintenance of the centrifugal compressor are cheaper, they have low power consumption at starting phase, higher reliability and longer lifetime.

Nowadays the demand for different calculation methods is enhanced, significant numbers of researches are in progress with applying these approaches in the mechanical engineering ([2], [6] and [7]). This is due to fact that high amount of cost, time and capacity can be saved by using well established and accurate design and analyses methods based on analytical, empirical or numerical solutions. The frontloading product development reconfigures the conventional design processes and several sampling phases can be omitted by the virtual prototyping.

Moreover, there is another aspect, according to which the modelling and simulation is more important in case of complex systems as gas turbines for example. The development namely, in general, can be classified by the two limiting cases based on the number of the products. The lower bound is called project related developments, which means that the effort turns to realize only one product (as a new building, a special ship or other machine for example), meanwhile the upper limit, the product based developments refer to the development of high number, sometimes millions of the products. The project related developments are characterised to be more costly, there are no sampling phases and there are tests by previously because the first product will be the final one in general. In contrast with that, the product based developments involve low cost products in general and measurements are often the cases in the sampling phases. The schematic about the range between the project and product related developments are shown in Figure 1. It is clear by the mentioned number of the products that the jet engines are more close to the project based developments, so the emphasize in design and developments are rather based on the modelling and simulation, which makes the design and also these system cost effective and guarantees the safety and reliability.






Project related developments	←-----→			Product related developments
				
Chain Bridge, Budapest [20]	Delivered Airbus A380 till May 2017 [21]	Built GE90 high bypass turbofan aircraft engines till 2014 [22]	Delivered new generation MB Actros since 2015 [23, 24]	Sold Jet Black iPhone 7 since 2007 till 2016 [25]
1 pcs	213 pcs	2000 pcs	100,000 pcs	1 billion pcs

Figure 1. The solution and product related developments

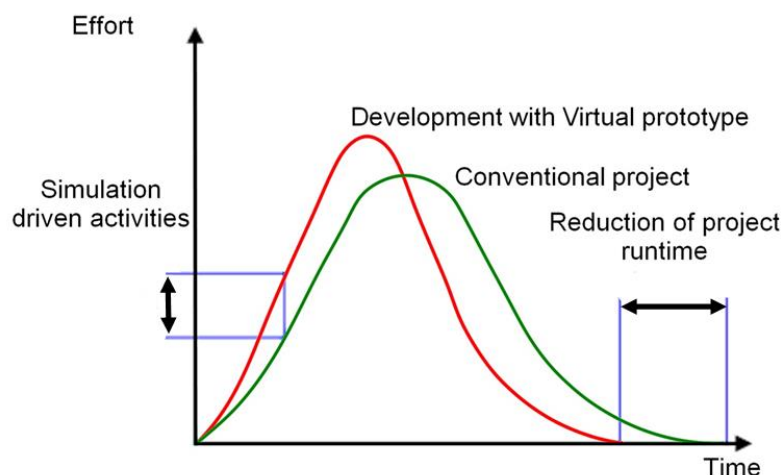


Figure 2. The impact of the virtual prototyping

In the most of the development processes, the available design variants are analysed by different calculation disciplines and design modifications are made if the characteristics are not matching

with the expected specifications or other constraints are violated. The presented loop is going on till the desired structure is available. The Figure 2 illustrates the impact of virtual prototyping on the time reduction and effectivity increment by using simulation driven product development. Of course, not the all design phases can be omitted by virtual prototyping. Measurements for validation purposes are indispensable to have at each design milestone.

The one of the main goals of the present research was to develop, apply, verify and validate aerodynamic development procedure of small jet engine corresponds to simulation driven product development.

DESIGN PROCESS OF THE GAS TURBINE

Developing a new engine is a difficult and complex task that can be separated into numerous steps, ranging from the definition of the engine specifications to the delivery and instruct of the very first engine. Although each engine manufacturer have own guideline for the design of gas turbine engine, a general representation of the development process can be found in [8] and it is shown in Figure 3. The design process is set up to five main phases following the specification state. The first one is the preliminary studies and the second one is the determination of the thermodynamic design point. They are followed by the aerodynamic design and analyses of the gas turbine components, mechanical design and finally the detailed design and preparation for production [8]. It is important to mention that the all steps have different crosschecking and confirmation loops in order to guarantee that design goals are achieved [8].

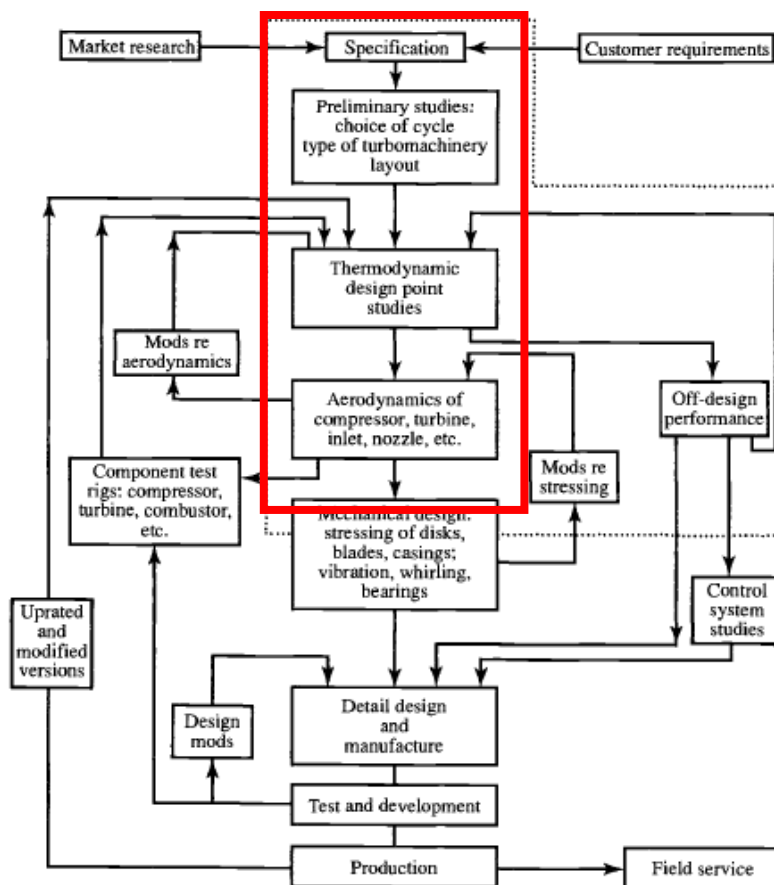


Figure 3. General design process for gas turbine engines [8]

Regarding the present research, the specification was given to redesign a small-sized research jet engine used for academic purposes.

The design process started with developing a mathematical model for the thermo-dynamical analyses by means of a concentrated parameter distribution type method in Matlab environment. This model was used to determine Thrust Specific Fuel Consumption – Specific Thrust map in the function of turbine inlet total temperature and total pressure ratio of the compressor.

Following the determination of the expected operational point, the main geometrical sizes of the engine and the necessary RPM were determined.

The next step of the process was the mean line and 3D design of the engine components as compressor, combustion chamber, turbine and nozzle, by which the all necessary dimensions for creating the 3D geometry of the jet engine were determined. This status is found in the box of “Aerodynamics of compressor, turbine, inlet, nozzle etc.” in Figure 3 and it is the last contribution of the design steps found in the red box, which contains the all design steps performed in the present work. However, the key word in the actually presented work is the virtual prototyping, which means that simulations (analyses) were completed following the detailed design and before manufacturing to crosscheck the correctness of the process and initiates design modification in case of need within the frame of the front loading design activities or design loop in other words.

GENERAL CONCERNS AND DESIGN ASPECTS

For designing the turbojet engine, it is essential to predetermine the method of calculating the characteristics in any particular cases for the specific values of the design variables. The design variables in this context mean the turbine inlet total temperature and the compressor total pressure ratio meanwhile the characteristics are the trust specific fuel consumptions in the function of the specific thrusts at previously imposed pressure losses and isentropic efficiencies. In order to find the corresponding ranges of the design variables, the pressure losses and isentropic efficiencies are estimated based on previous literature research close to the expected operational condition, and for the simplicity, they are kept to be constant in each point to be calculated. The turbine inlet temperature has strong effect on the specific thrust. In general, keeping the engine as small-sized as possible for a given thrust is possible by having the highest maximum allowable value of TIT with concerning the metallurgic reasons as limitation. Furthermore, the increase in pressure ratio of the compressor will obviously cause decrease in the specific fuel consumption. Therefore increasing specific thrust by increasing the total temperature at turbine inlet section is more essential in case of small engine when a decrease in the drag and weight is required. At constant value of turbine inlet temperature, increasing pressure ratio first leads to rising specific thrust and finally decreases that. The maximum specific thrust can be determined by the maximum allowable turbine inlet temperature and optimal pressure ratio of the compressor belongs to the maximum thrust. It is obvious that for any certain/smaller value of pressure ratio and temperature of turbine inlet section, the specific thrust is decreased and the specific fuel consumption is increased.

Regarding the turbine inlet total temperature and compressor total pressure ratio, the following aspects can be considered. High turbine inlet temperature can cause to increase the complexity of the structure and cost due to the application of cooled turbine blades and expensive alloys. Additionally, it is important to note that increasing pressure ratio enhanced engine weight, complexity and cost due to the need for more stages and multi spool configurations in extreme. These conditions are opposite with the needs, where the goal is to create a low cost academic jet engine.

REDESIGN PROCEDURE OF THE TURBOJET ENGINE

The origin of the presently redesigned jet engine is TSz-21 starter gas turbine used for MiG-23 and Szu-22 Russian fighters. The TSz-21 engine has been modified to be a research jet engine from 2005–2008 but it is still under development with especial care for control [10].

The goal of the actual work is to introduce, apply and verify a design process for small-sized jet engine and analyse the results by using CFD method with validation by the available measured data.

The jet engine under interest is a compact lightweight and possibly low-cost system that is adequate to create around 330 N thrust at steady state ambient conditions for academic and research purposes.

The following subchapters introduce the applied design methods as thermo-dynamical cycle analyses with determination of the design point, mean line and 3D design of the compressor, combustion chamber, turbine and nozzle.

Thermodynamic analysis of the research turbojet engine

The mathematical model was developed and used to determine the operational points and performances of the small turbojet engine. The method is introduced in detail in [9]. The following design criteria and assumptions are made in the thermo-dynamical model. Ambient pressure and temperature of air are 99,000 [Pa] and 300 [K] respectively, the fuel is assumed to be liquid kerosene with a heating value of 42,700 kJ/kg and nozzle is unchoked. The considered parameters of total pressure recovery factors and efficiencies are found in Table 1.

Total pressure recovery factors of combustion chamber (r_{cc}), and intake duct (r_d) and efficiencies of the cycles as mechanical (η_m), nozzle (η_n), burning (η_b), compressor ($\eta_{c,s}$) and turbine ($\eta_{t,s}$) isentropic respectively							
Parameters	r_{cc}	r_d	η_m	η_n	η_b	$\eta_{c,s}$	$\eta_{t,s}$
Input data	0.94	0.96	0.99	0.95	0.96	0.7	0.8

Table 1. Specified parameters of turbojet engine by the previous experiences

The next step is to determine the expected design point of the jet engine. Hence, first, the performance map of the engine has been created, where the thrust specific fuel consumption values are plotted in the function of the specific thrust, turbine inlet temperature and total pressure ratio of the compressor. By this way, the effect of compressor pressure ratio on air mass flow rate is excluded; the variation in compressor pressure ratio does not change the mass flow rate

across the engine at the same temperature (unchoked engine operation). The outputs of the cycle analyses are used to determine the points of the functions according to (1-2) respectively [18].

$$T_s = (1 + f_{cc})(V_9 - V_0) + \frac{(1+f_{cc})}{\rho_9 V_9} (p_9 - p_0) \quad (1)$$

$$SFC = \frac{f_{cc}}{T_s} \quad (2)$$

The performance map is shown in Figure 4. For designing the jet engine, the basic thermo-dynamic parameters to be determined by the designer are the compressor total pressure ratio (π_c) and turbine inlet temperature (T_{04}).

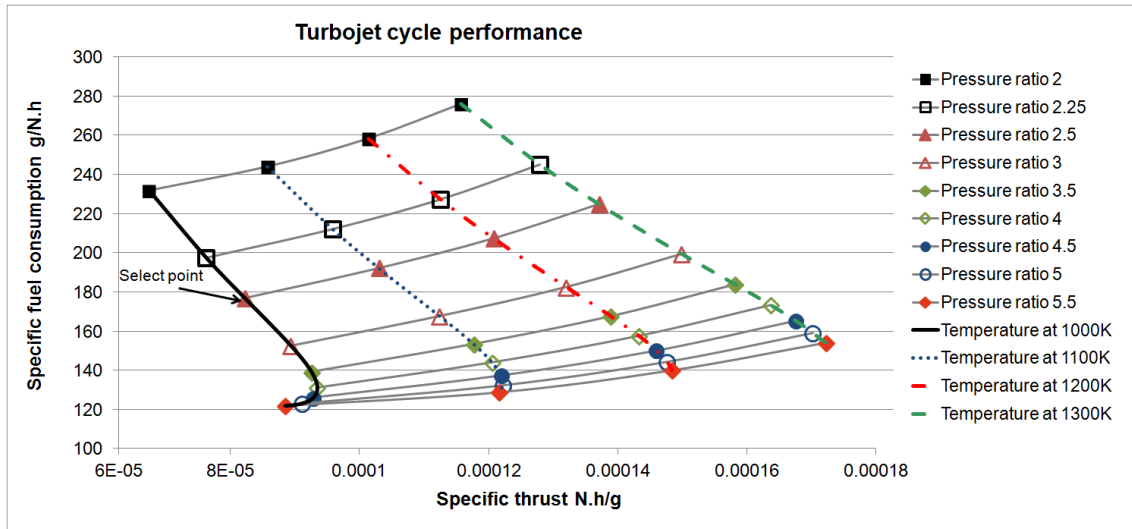


Figure 4. Cycle performance curves

A total pressure ratio 2.5 was selected in the present case to be a reasonable compromise within the investigated range. As to achieve high pressure ratio, it is required to consider higher dimensions, performances and/or advanced production technology, which cannot be afforded by university purpose in the recent conditions. 1000 K turbine inlet temperature was selected with considering that there is limited access for using high-tech cooling technology and advanced materials for the turbine blades. The specific thrust was 309.6 Ns/kg at this point.

So, by having the specific thrust and thrust of the research jet engine it can be able to determine the mass flow rate by the following way:

$$\dot{m}_{air} = \frac{T}{T_s} = \frac{330}{309.6} = 1.065 \frac{kg}{s} \approx 1 \frac{kg}{s} \quad (3)$$

The real thermo-dynamical cycle of the engine in T-s diagram is plotted in Figure 5. The red curves (with smaller thickness) represent the constant pressures. The processes between the engine states denoted by numbers are plotted by thicker lines. This visualization effect is the reason of constant pressure lines goes below the process line in case of pressure decrement just after section "3".

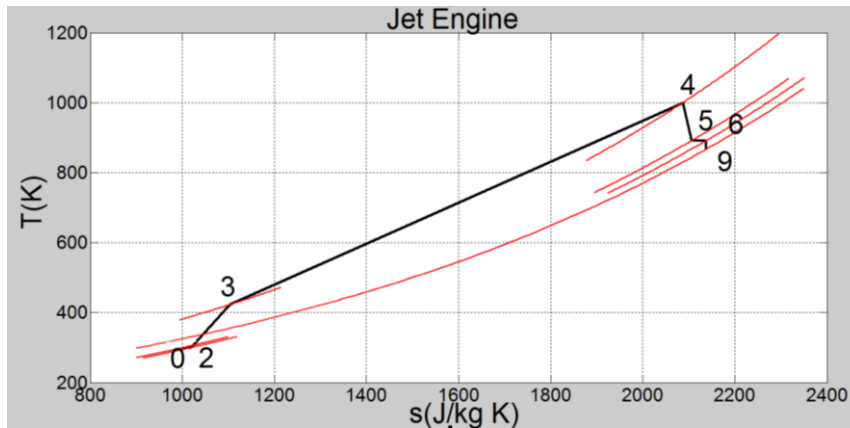


Figure 5. The T-s diagram of research jet engine with single spool

After completing the thermodynamic analysis based on the required design specifications, the next step is to determine the main geometrical sizes of the engine components and the RPM belongs to design point according to [18].

Compressor design and analysis

Centrifugal compressors are utilized most prevalently in gas turbine engines, gas transportation industry and turbochargers of internal combustion engines [11]. Several researches and developments have been completed with relating of centrifugal compressors as [12]-[15] for example so far.

For a small, compact and light-weight jet engine with 2.5 total pressure ratio, the selection of a single-stage centrifugal compressor is reasonable. Using the design data from the thermodynamically cycle analysis and the main geometrical sizes of the jet engine with the engine speed, the impeller and diffuser were designed by the procedure outlined in [16]. The equations used here are based on the common thermodynamic and aerodynamic principles in a mean stream line. The input data of the mean line design for the centrifugal compressor are given in Table 2. There are three variables amongst them as B_1 , $\eta_{r,s}$ and C_{pD} , which represents the boundary layer blockage, isentropic efficiency of the rotor and pressure coefficient of the vanned diffuser respectively and these are determined by experiences [16]. The output of the process is the main dimensions of the compressor, the velocity triangles and the thermodynamical parameters.

Input parameters of the centrifugal compressor			
p_0	99,000 [Pa]	B_1	0.057 [-]
T_0	300 [K]	N	43,000 [rev/min]
\dot{m}	1 [kg/s]	$\eta_{r,s}$	0.78 [-]
α_1	0 [deg]	C_{pD}	0.65 [-]
r_{1h}	0.0022 [m]	z	20 [-]
r_{1t}	0.0052 [m]		

Table 2. Design specification and the results of the centrifugal compressor

The 3D model of the assembly was prepared according to the main dimension, which is shown in Figure 6 in the meridional view.

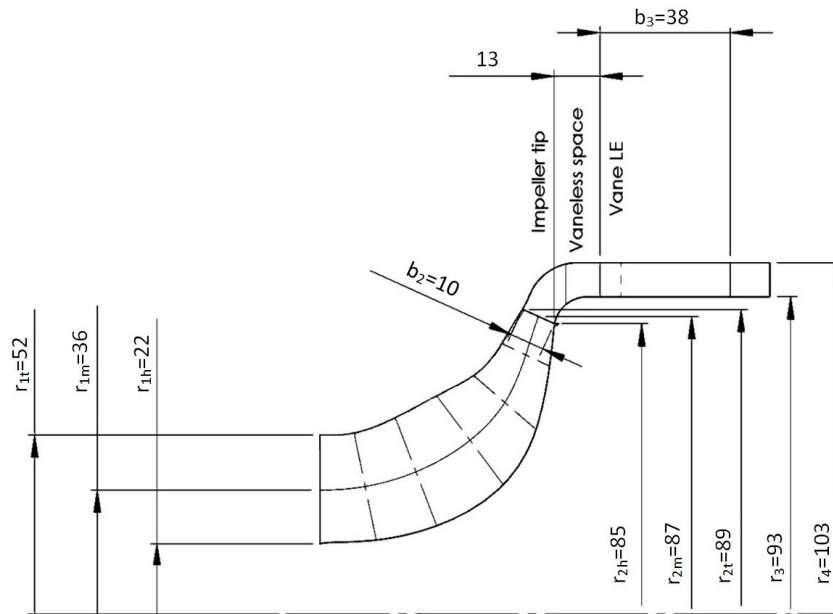


Figure 6. Meridional view of centrifugal compressor (the dimensions are in [mm])

Design aspect of the combustion chamber

The combustion chamber has the challenging task of burning certain amount of fuel that is supplied through the fuel burners with wide range of volume of air. The air leaving the compressor goes through the combustors, expanding and accelerating to give a smooth stream of uniformly heated gas at all conditions required by the turbine. The fuel is burned almost stoichiometrically with only 25 to 35 percent of total air entering [17] and it is 28 % in the present case ($\dot{m}_{fcc} = 0.019 \frac{kg}{s}$, $L_0 = 14.72 \frac{kg}{kg} \Rightarrow \dot{m}_{air,st,cc} = \dot{m}_{fcc} L_0 = 0.2797$), the combustors in order to keep the turbine inlet temperature down to permissible limits. As a result, combustion must be completed without causing high pressure loss and taking into consideration the huge heat release for the limited space existing. In providing adequate turbulence and mixing, a total pressure loss changing from about 2 to 9 percent of the air pressure at which it goes through the chamber [17].

For many years the combustion has had less capability to theoretical treatment in comparison with other parts of the gas turbine and any development software involved some trial and error. With high cycle temperature of modern gas turbine, mechanical design stays complex task and need for improvement of technical development is obvious. Concerning the industrial gas turbines they have a certain range of usable types of fuel amongst them natural gas is included frequently beside the liquid based hydrocarbons [17].

Combustion chambers can be distinguished based on their structure. Regarding flow direction, reverse-flow and one-directional flow combustion chambers exist.

The reverse-flow combustion chambers have the advantage of obtaining shorter gas turbine design, because the flow path is shortened by half in one direction as the combustor is located to sit on perimeter of the compressor and turbine. Thus this design does not require so improved shaft materials and bearing design compared to the one-directional flow combustion chambers. Due to this, the reverse-flow combustion chambers are basically applied on older gas turbines,

however, where a short and compact design is required, this combustion chamber is still applied nowadays. As a disadvantage, reverse-flow combustion chambers have high pressure losses compared to one-directional chambers. Furthermore, due to the noticeable cross section, reverse-flow combustion chamber produces high aerodynamic drag, thus they are very rarely used in aircraft propulsion systems.

Although gas turbines, which are applied with one-directional flow combustion chambers are longer, hence better shaft materials and improved bearing designs are required, due to the lower cross section and better total pressure recovery factor and burning efficiency; they are more widespread in aviation industry.

Regarding the one-directional flow combustion chambers, there are three main types of the structure can be distinguished. They are the multiple can, can-annular and the annular type combustion chambers. All of the three kinds of combustors have the recirculation, burning and dilution zone. First of all, fuel is partially burned in the recirculation zone. But there is some fuel, which is not completely burned, so the remainder of fuel is completely burned in the burning zone. The hot gas is then mixed in the dilution zone with the cooling air and provides a suitable inlet temperature for the turbine section. One part of the cooling air works on the principle of film cooling, it separates hot working fluid from the walls of the combustor; hence higher operating temperatures can be allowed. Furthermore, appropriate application of cooling air contributes to flame stabilization and more even mixture distribution while proceeding to the turbine inlet cross section [17].

The combustion chamber design is a complex and challenging task in small gas-turbine engines due to the size limitation by means of couplings the compressor and turbine, typically constructive limitations on shaft length and diameter. These requirements have focused also in the present case to highlight a particular type of combustor, the annular combustion chamber. It is essential to mention that this kind of chamber is ideal because of “clean” aero-dynamic layout results in a compact unit of higher burning efficiency than other combustor types. In development of turbojet engines, the use of annular combustion chamber is confined to low pressure ratio, so for small gas turbines would seem to be more appropriate to apply an annular combustion chamber [17].

This kind of combustors includes a single flame tube, completely annular form, which is consisted in an inner and outer casing. At the front of compressor and the back of the turbine nozzle the chamber is open. The holes, which are placed in the shroud section of casing, allow the secondary air to enter the combustion chamber and guide the flame away from the shrouds to preserve the wall of the combustion chamber at a permissible relatively low temperature. The fuel at this type of combustor is entered through sequences of nozzle at the upstream end of the flame tube. This kind of combustor has the benefit of being able to use smaller cross section, achieve smaller pressure loss and 25% smaller structural mass if compared with can-type [17]. The other advantages of this kind combustor that the limited space available is used more effectively, allowing better mixing of the fuel and air within a fairly simple structure. Also more uniform combustion than in can type combustion chamber, better flame propagation and for the same output, it is 75 % shorter in general than the can-annular type chambers of the same di-

ameter, hence less weight, less production and maintenance cost may be achieved [17]. In addition there is less wall area needed in comparison with other types, consequently less cooling air, better combustion efficiency and less pollution are resulted.

Based on the all characteristics and consideration described above, for a small-scale academic gas turbine, due to its advantageous properties, an annular-type combustion chamber was selected for design. The combustor was created in the CAD model. The basic geometry of the gas turbine combustor is shown in the Figure 7. The primary inlet air is guided by the air a swirling velocity component. The injection diameter of the fuel is 0.8 mm. The secondary air is injected in the combustion chamber across 6 mm bores. The dilution bore diameters are 12 mm.

Turbine design and analysis

The short description of the turbine unit design has been introduced in the present subchapter.

The already calculated data came from the thermodynamic cycle analysis, from the computation of the main geometrical sizes of the engine and from the number of revolution were used for turbine design. The applied design process is based on [18] and carried out by using a one-dimensional procedure at the mean radius of turbine with the main goal of relating connection between the power, thermodynamical variables and velocity triangles. The 3D blade geometries in CAD software were prepared after considering blade twisting and profile generation.

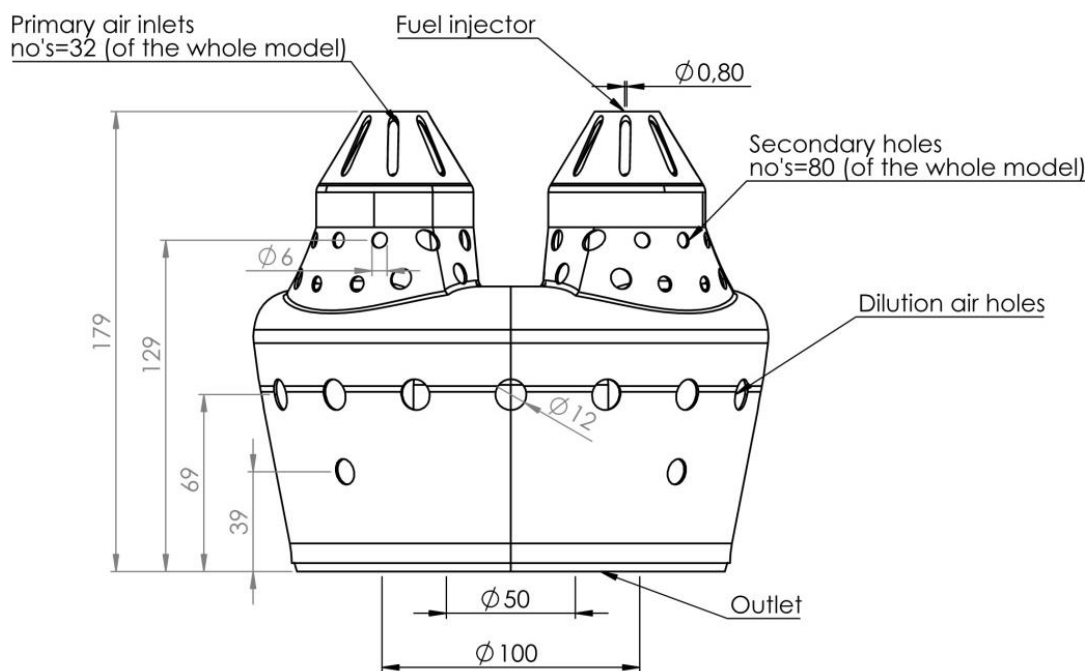


Figure 7. Basic geometry of the annular-type of combustion chamber (the dimensions are in mm)

The more detailed introduction of the design process is the following. The input parameters for the mean line design of the turbine were the inlet total pressure and temperature, mass flow rate, RPM, pressure ratio of the turbine, enthalpy drop and target efficiency. The number of revolution was the same as it was used in the centrifugal compressor design of course and the static structural stress analysis was completed by using simple analytical equation to check the integrity of the turbine blades. In addition, during the design of turbine some values were prescribed

as design parameters. These were the degree of reaction, speed factor and stage loading. The output or calculated parameters of the design process were the stage number, the number of the blades, velocity triangles and the thermodynamical parameters in the each section of the stage. Constant degree of reaction blade twisting was applied in the process to guarantee the expected advantages of radial equilibrium in 3D. Finally, the blade profiles were created by using the method of camber line preparation from profile catalogue and the geometrical model of the turbine stage in 3D was created in Solid Edge environment.

Input parameters of axial turbine			
r°	0.2 [-]	p_0	244930 [Pa]
φ_s	0.98 [-]	T_0	1000 [K]
φ_r	0.94 [-]	π_T	1.96 [-]
ε	0.96 [-]	N	43000 [rev/min]
D_{1m}	0.1445 [m]	A_2	0.0158[m ²]
A_1	0.016 [m ²]	\dot{m}	1[kg/s]

Table 3. Design specification of turbine

The blade profile and velocity triangles at the mid-section plane are shown in Figure 8.

Nozzle design

A simple convergent-shaped exhaust nozzle was designed by featuring of an effective exit area of 75 cm², which makes the nozzle unchoked at the design point.

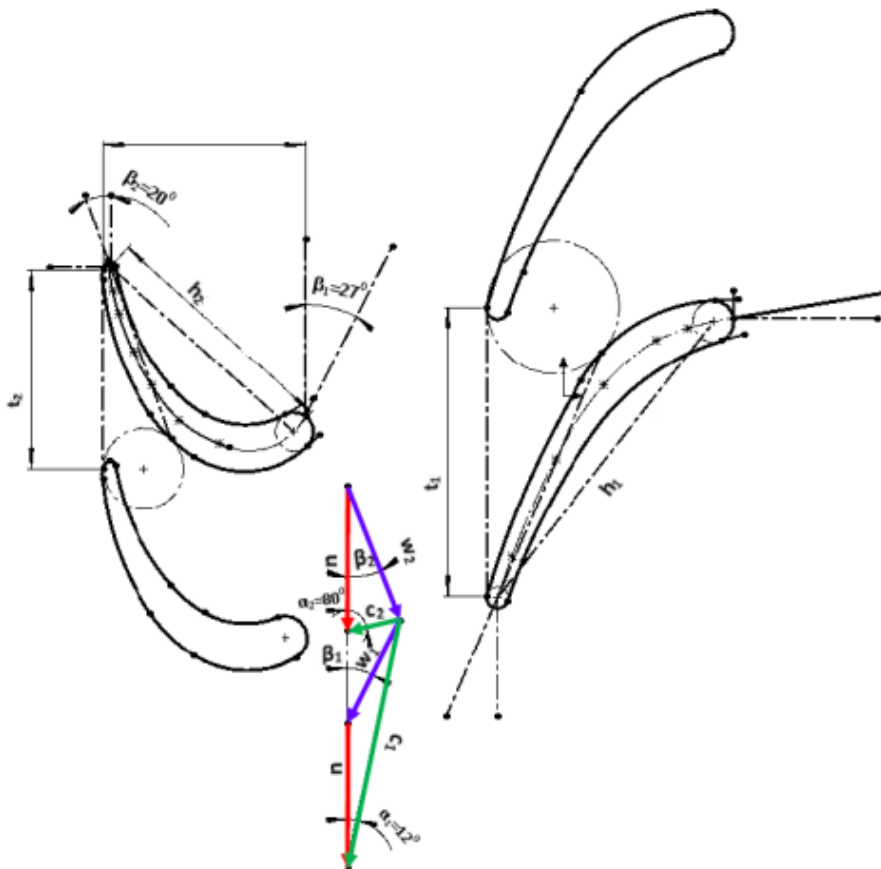


Figure 8. The velocity triangles with the turbine rotor and stator blade profiles at the mean section

CFD ANALYSIS OF THE RESEARCH JET ENGINE

The all components of the research jet engine were available in 3D CAD format till the end of the design process. The next step of the investigations was to crosscheck how the all components working together and how this operation fulfil the design goals. Hence, 3D CFD simulation was prepared and completed for the entire model after creating the flow field by using the solid components. The model preparation and the results of the numerical analysis are discussed in the present chapter. The 3D model was created in Solid Edge software based on the geometry output described in chapter 4 and measured data from the available structure. The 3D geometry of the assembly is found in Figure 9.

The flow field was prepared from the 3D structure by Boolean operation. The solid domains were subtracted from a reasonable big oversized volume to get the flow field in the intake channel, in the compressor, in the combustion chamber, in the turbine and in the nozzle. Only the one quarter flow domains were considered by using rotational periodicity boundary conditions between corresponding surfaces to save computational cost, time and increase the accuracy by means of allowing higher cell number. The used flow domain is shown in Figure 10. The Figure 11. represents the plane, at which the simulation results will be shown in the last part of the present chapter.

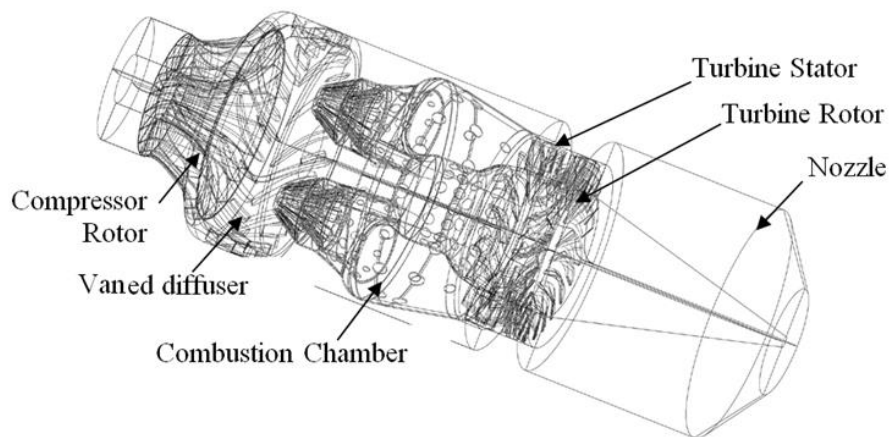


Figure 9. Assembly and the main component of the research jet engine

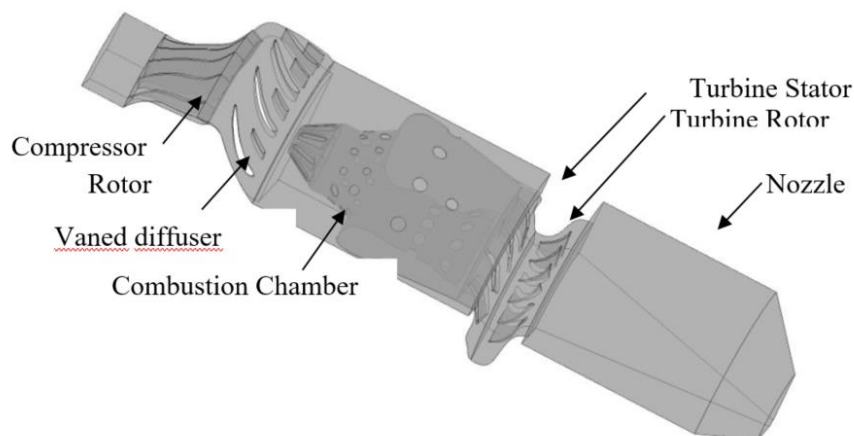


Figure 10. One quarter flow field of the research jet engine with the main components

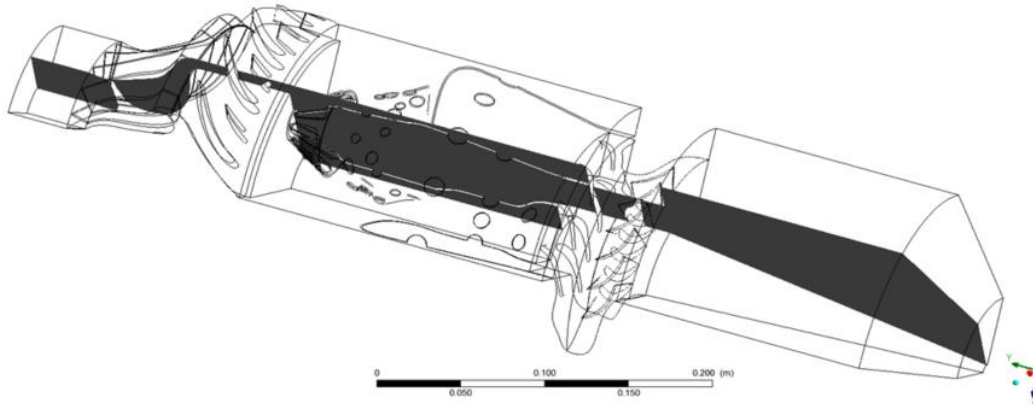


Figure 11. Flow field of a quarter research jet engine and the plane for the representation of the results

The numerical mesh was designed to apply local mesh refinement at the high gradient flow conditions and to guarantee the completeness of y^+ to be 30-300. It was a general expectation that results should be mesh independent by 5 % maximum allowing differences in the thrust. The final mesh was built up from 4799728 elements and it contained 2067312 nodes. The 32 GB RAM memory was reached by the simulation. The final mesh configuration is shown in Figure 12.

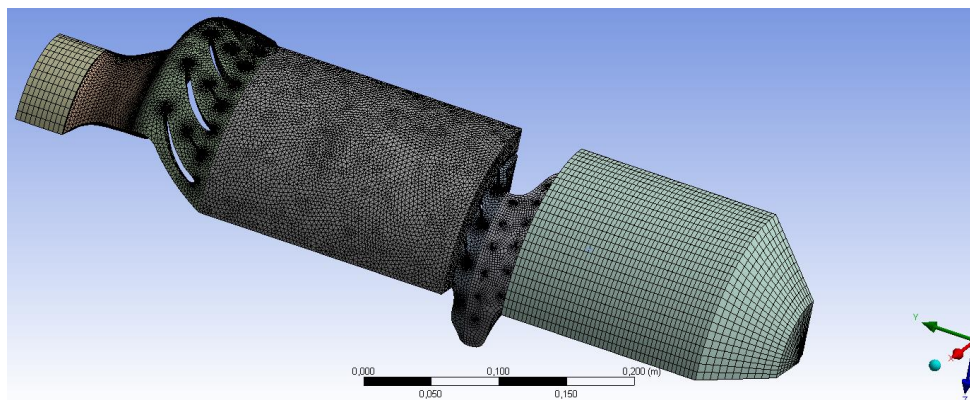


Figure 12. The final mesh for the one quarter flow field of the research jet engine

The material properties of the incoming air as ideal gas were $\gamma = 1.4$ and $R = 287.058 \text{ J}/(\text{kgK})$. The reference pressure of the domains was 99,000 Pa. The ambient air enters in the jet engine and the hot gases expand in the environments. Hence 99,000 Pa total pressure and 300 K total temperature with normal flow direction into the inlet surface of the intake flow channel were defined as inlet boundary condition. 1 bar static pressure was defined as outlet boundary condition. 43,000 RPM rotational speed turned the rotating flow domain of the compressor and turbine. Table 4. shows the all used boundary conditions.

Figure 13. provides an overview about the type and the location of the used boundary conditions. The heat transfer coefficient $8 \text{ W}/(\text{m}^2 \text{ K})$ corresponded to the stationer ambient air with 300 K temperature on the outer walls were applied for considering the free convection.

Inlet air			Inlet fuel		Outlet
p_0 [Pa]	T_0 [K]	N [rev/min]	V [m/s]	T_0 [K]	Opening pressure [Pa]
99,000	300	43,000	12	300	99,000

Table 4. The applied boundary conditions

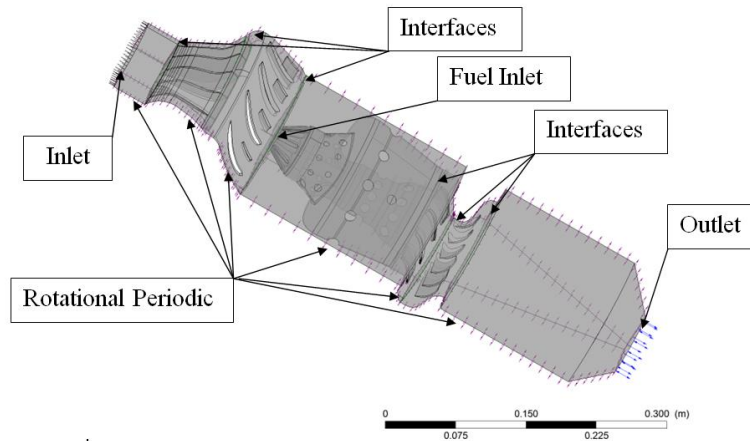


Figure 13. The used boundary conditions and interfaces in the CFD simulation

The considered governing equations were the conservation of mass, momentum and energy together with other supplementary equations for the turbulence and combustion. The standard k-epsilon turbulence model and P-1 radiation model were used in this analysis [19].

Regarding the combustion modelling, non-premixed combustion modelling with the PDF-mixture fraction model was used. In the non-premixed combustion, the fuel and oxidizer enter separately in the reaction zone. The PDF Flamelet combustion model can handle chemical reactions, which go through in a short time in a non-premixed turbulent fluid flow. The generated Flamelet library for Jet A is large since it includes all the possible species that can exist in the Jet-A combustion. Simulations with this library take much computational time and computer resources. Even the required time to load this library at the beginning of each simulation is more than forty minutes. In order to save time the species of the library are reduced to H, O₂, OH, O, H₂, H₂O, CO, CO₂, N₂, C₁₀H₂₂, TMB C₉H₁₂ and N₂. The Table 5. represents the list of applied models to be used in this simulation for combustion modelling.

Advection scheme	High resolution
Primary breakup	Blob Method
Combustion	PDF flamelet
Turbulence model	K-Epsilon
Thermal radiation model	P1
Heat transfer	Ranz Marshall
Drag Force	Schiller Naumann
Turbulence model discretization scheme	First order
Liquid phase	Lagrangian Particle Tracking

Table 5. The applied methods for combustion modelling

The simulation was converged. The imbalances reached the 1% limit after 1000 iteration steps.

The simulation results are shown in the next part of the chapter. The qualitative results are plotted in the plane denoted by Figure 11. and they are presented in Figure 14-16. These distributions are plausible; they are fit to the design expectations and measured values discussed in the next chapter.

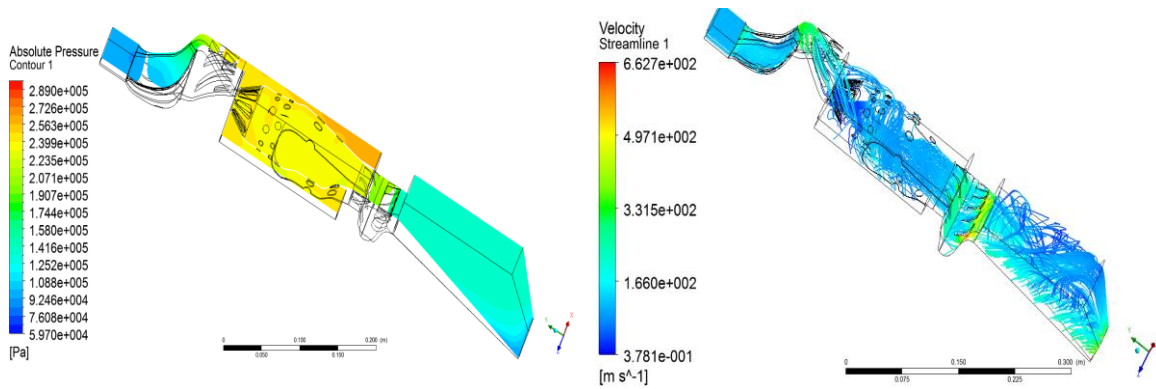


Figure 14. Streamlines (coloured by the velocity magnitude – left figure) and absolute static pressure distributions (right figure) in the meridional plane of the research jet engine

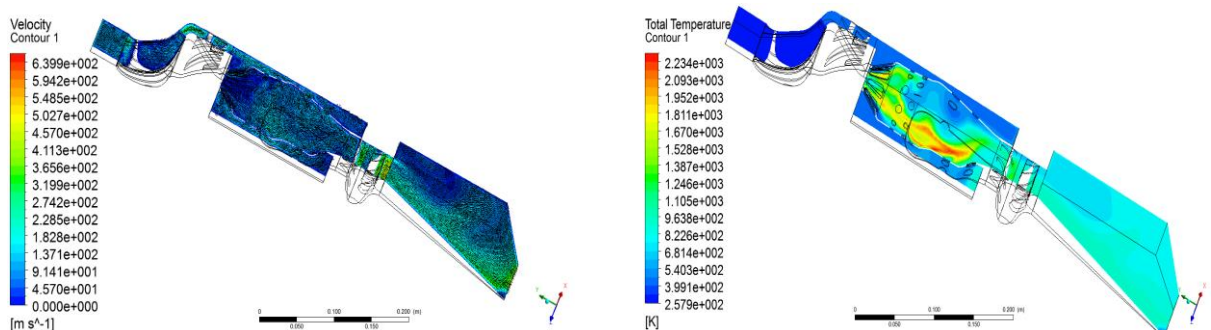


Figure 15: Velocity vectors (left figure) and total temperature distribution (right figure) in the meridional plan of the research jet engine

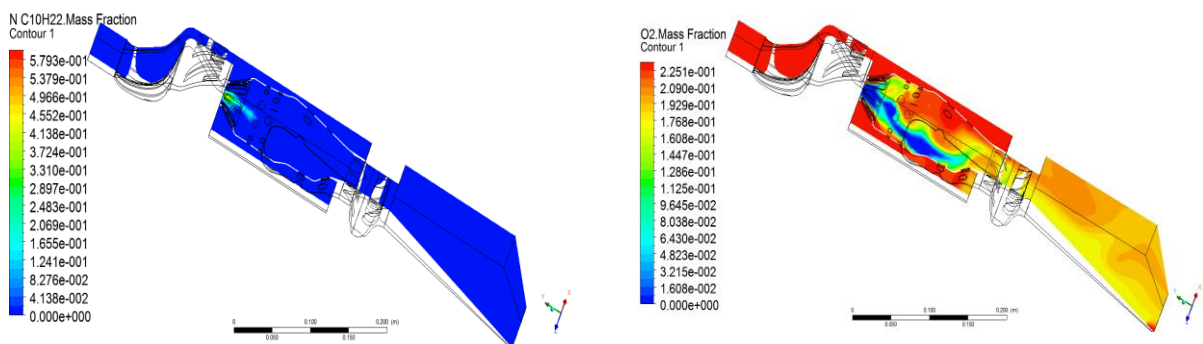


Figure 16. Mass fraction of the fuel (left figure) and O_2 (right figure) in the meridional plane of the research jet engine

DISCUSSION, CONCLUSION AND VALIDATION OF THE RESULTS

There are two goals of the present chapter. The one of them is to compare the design targets and the parameters, which were calculated by the engine design with the results of the CFD analysis. The second one is to compare the CFD data with the results of the available measured values [19]. The thermodynamical parameters - if they were available - as total temperature, total pressure, static temperature and static pressure are presented along the engine length for

results of the thermodynamical cycle analysis, mean line design, CFD simulation and measurement in Figures 17-20.

The total temperature of each stage provided by cycle analysis, mean line design, CFD and measurements at the interface regions of the assembly are shown by empty blue circles, black stars, empty red squares and empty green triangle symbols respectively (see Figure 17). As expected, the total temperature at the inlet section of the nozzle and the compressor inlet is the same and equal to ambient total temperature. Then, it becomes slightly higher, quite above 400 K at the compressor exit. The total temperature increases dramatically to about 1000 K in the combustion chamber and finally it declines at the end of the turbine and the nozzle section. The maximum relative difference between the mean line design and CFD data is 2% meanwhile the average relative deviation between the investigated points is 0.64%. The maximum relative difference between the cycle analysis and CFD data is 2% and the average relative deviation between the points is 0.89%. Concerning the CFD and measured total temperatures, the maximum relative difference between them is 3% and the average relative deviation between their values is 1.19%.

Figure 18. shows the calculated and measured static temperatures in the function of the engine length similarly than it was mentioned in the previous paragraph except for the thermodynamic data, because only the total quantities were considered in the cycle analysis. The calculated mean line design and CFD results match well with each other similarly than before, only slight difference can be observed between their and measured data. The maximum relative difference between the outputs of the mean line design and CFD simulation is 2.2% and the average relative deviation between the investigated values is 0.68%. The highest relative difference between the available measured and CFD data is 3.9% and the average relative deviation between the investigated static temperatures is 1.67%.

The total pressure at the compressor inlet is 99 kPa. It is boosted by the compressor to 250 kPa before the combustion chamber (see Figure 19.). Afterwards, it expands to the atmospheric pressure in three steps. First, it decreases slightly going through the combustion chamber. Then the flow enters into the turbine and the pressure drops to 110 kPa. Afterwards, the pressure decreases until the end of the nozzle as it is shown in Figure 19. It can be seen that the CFD model gives greater total pressure in the last two sections of the engine (at the turbine and nozzle end). The maximum relative difference between the thermodynamic cycle and CFD data are 4% and the average relative deviation between the points in the entire range is 2.1%. Similarly, the maximum relative difference between the results of the mean line design and CFD total pressure is 5% meanwhile the average relative deviation between the points is 1.3%. Concerning the CFD and measured total pressures, the maximum relative differences between them is 5% and the average relative deviation between their values is 2.2%.

Plotting the measured static pressure along the length of the engine, as it is shown in Figure 20, it provides information also about the usability and accuracy of the design process and model. The thermodynamic cycle analysis has no static parameters, because it uses total ones only. The maximum relative difference between the results of the mean line design and CFD data are 7%

and the average relative deviation between their investigated points is 3.8%. The highest relative difference between the available measured and CFD data is 5% and the average relative deviation between the investigated static pressures is 3.2%.

330 N thrust was the goal function of the design and 345 N thrust was resulted by the CFD analysis. The relative difference between them is 4.54%, it is below the 5% limit, so the used design process is acceptable in engineering point of view. The measured thrust was not used in the present assessment because of uncertainty communicated by the authors [10 and 19].

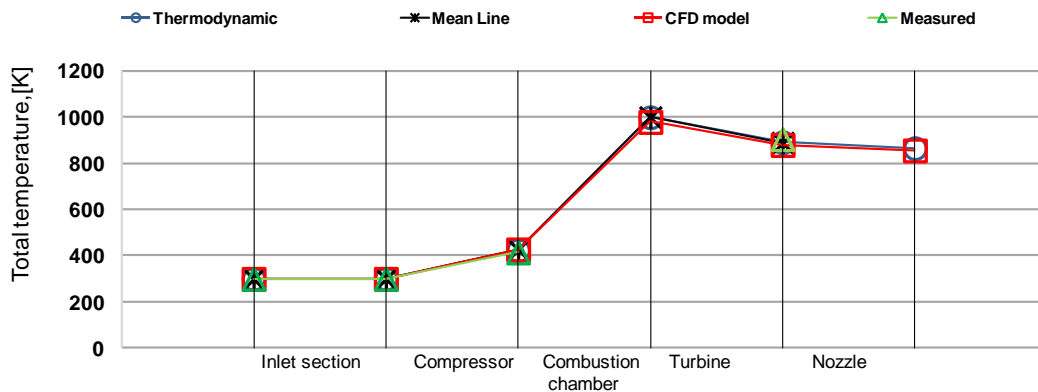


Figure 17. Total temperatures - if they were available - in the function of engine segments at thermodynamic analysis, mean line design, CFD analysis and measurement [19]

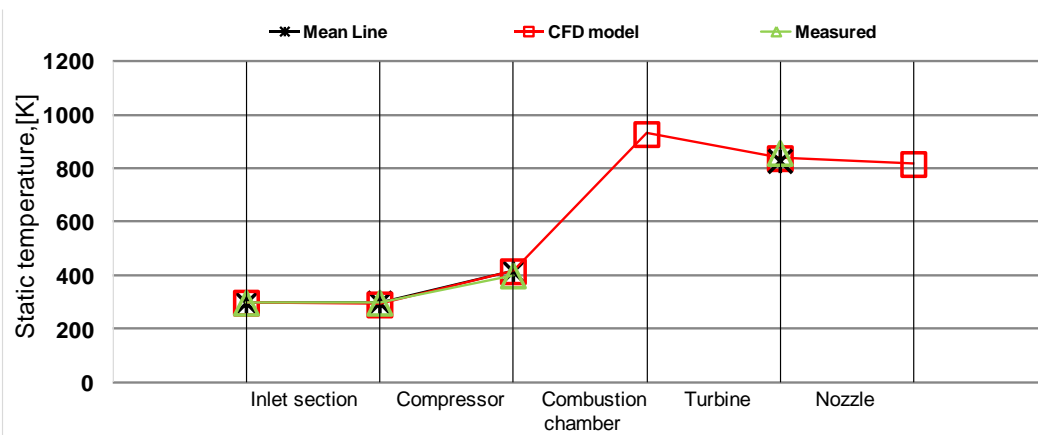


Figure 18. Static temperatures - if they were available - in the function of the engine segments at mean line design, CFD analysis and measurement [19]

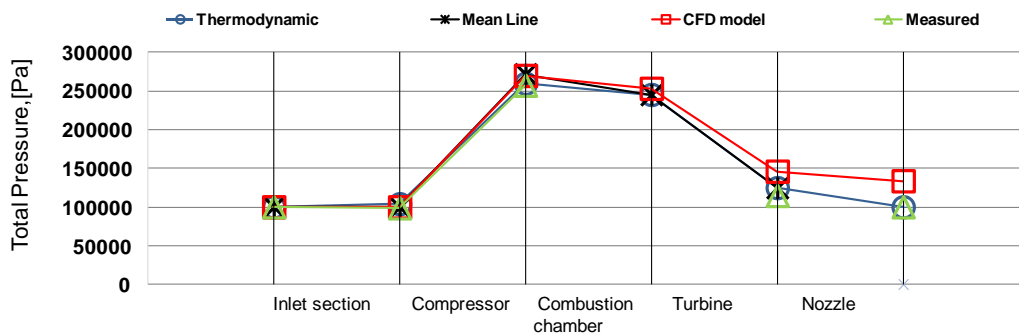


Figure 19. Total pressure values - if they were available - in the function of engine segments at thermodynamic analysis, mean line design, CFD analysis and measurement [19]

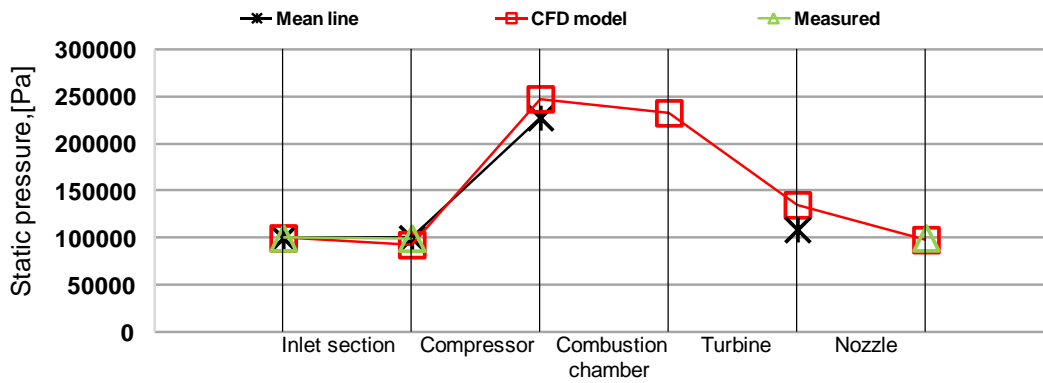


Figure 20. Static pressures - if they were available - in the function of engine segments at mean line design, CFD analysis and measurement [19]

CONCLUSION

The aerodynamic redesign of the small research jet engine has been introduced in the present paper. The considered engine was a starter gas turbine originally, which was used for MiG-23 and Szu-22 Russian fighters. It was reconstructed to be a propulsion system by Dr. Beneda and dr. Pásztor [10]. The present redesign process started with imposing the operational point of the engine to provide 330 N thrust at stationary conditions. The thermodynamically cycle of the engine process was determined with viscous flow assumption and condition dependent material properties for determining specific thrust and thrust specific fuel consumption. After making decision about operational point and having the thermo-dynamical cycle states, the main geometrical sizes of the research jet engine were determined and rotational speed was imposed. Mean line design of the compressor and turbine were completed with considering the available thermodynamic results, main geometrical sizes and RPM. Following the application of the constant degree of reaction along the radius for twisting, the turbine blade profile was constructed. The 3D CAD models were prepared by using the available and determined geometrical data, which were the outputs of the design. The one quarter part of the created 3D model is used to generate the 3D model for CFD simulation in order to crosscheck that how the design goals were realised.

There are two ways of checking the result of the design. One of them is to compare the engine design parameters (given by thermodynamic cycle analysis and mean line design) with CFD analysis and second one is to evaluate the results of the CFD analysis with available measured data. The outcomes of these investigations were the following. The relative average difference between the CFD and the thermodynamic cycle analysis is 0.89% for the total temperature and 2.1% for total pressure. The relative average difference between the CFD and the mean line design is 0.64% for total temperature and 0.68% for static temperature. Similarly, the relative average difference between the CFD and the mean line design is 1.3% for the total pressure and 3.8% for static pressure. Available measured data is used for validation of the result of the research jet engine. The relative average difference between the available measured data and the CFD analysis in case of total temperature is 1.19% and 1.67% for static temperature. The

relative average difference between the available measured data and the CFD analysis in case of total pressure is 2.2% and 3.2% for the static pressure.

The value of the thrust for the research jet engine is 345 N at CFD analysis. The relative difference between design value and the resulted thrust is 4.54%, which is acceptable in engineering point of view.

ACKNOWLEDGEMENTS

This work was supported by Hungarian national EFOP-3.6.1-16-2016-00014 project titled by "Investigation and development of the disruptive technologies for e-mobility and their integration into the engineering education".

REFERENCES

- [1] Voskuilj, M., Rohács, D., Rohács, J., and Schoustra, R-J.: Preliminary Evaluation of the Environmental Impact Related to Take-off and Landings Supported with Ground-Based (MAGLEV) Power, *Journal of Aerospace Operations*, Vol. 2, No, 3-4, pp. 161-180, 2013.
- [2] Bera, J., Pokorádi, L.: Monte-Carlo Simulation of Helicopter Noise, *Acta Polytechnica Hungarica*, Vol. 12, No. 2, pp. 21-3, 2015
- [3] Beneda, K.: Development of a Modular FADEC for Small Scale Turbojet Engine, SAMI 2016 - IEEE 14th International Symposium on Applied Machine Intelligence and Informatics - Proceedings, art. no. 7422981, pp. 51-56, 2016.
- [4] Beneda, K., Simongáti, Gy., and Veress, Á.: "Járművek hő- és áramlástechnikai berendezései I," Typotex Kiadó, Budapest, Chaps.3, pp.73-82, 2014.
- [5] Chu, H.H., Chiang, Hsiao-Wei.: Aerospace Technology Development – Small Gas-Turbine Development, ROC: Aerospace Development Planning, National Science Council, Taiwan, pp. 4-22, 1996.
- [6] Beneda, K.: Dynamic Nonlinear Mathematical Model of Active Compressor Surge Control Devices, Proceedings of the 11th Mini Conference on Vehicle System Dynamics, Identification and Anomalies (VSDIA), Budapest, pp. 583-591, ISBN: 978-963-313-011-7, 2008.
- [7] Hargitai, Cs.: Effect of Parameters of Inland Vessel Semi Empirical Motion Equations on Transient Motion Phenomena, in Proceedings of the TVL: Second Scientific Workshop on Transport, Vehicle and Logistics organized by the PhD Schools of the Faculty of Transportation Engineering and Vehicle Engineering, 2012.
- [8] Mattingly, J. D., Boyer, K. M.: Elements of Propulsion: Gas Turbines and Rockets, Reston, Virginia, Second Edition (AIAA Education), ISBN: 978-1624103711, 2006.
- [9] Zare, F., Veress, Á.: Development and Verification of an Improved Thermodynamical Model for Single Spool Jet Engines, in *Repüléstudományi Közlemények 2014*, Szolnok, pp. 539-551, 2014.
- [10] Beneda, K., Pásztor, E.: A TKT-1 Kisméretű, Oktatási és Kutatási Célú Gázturbinás Sugárhajtómű Első Tíz Éve, in *Repüléstudományi Közlemények 2015/3*, Szolnok, pp. 117-132, 2015.
- [11] Kalabic, U., Kolmanovsky, I., Buckland, J., and Gilbert, E.: Reference and Extended Command Governors for Control of Turbocharged Gasoline Engines Based on Linear Models, *Control Applications (CCA)*, 2011 IEEE International Conference, IEEE, pp. 319-325, 2011.
- [12] Botros, K. K.: Single Versus Dual Recycle System Dynamics of High Pressure Ratio, Low Inertia Centrifugal Compressor Stations, *Journal of Engineering for Gas Turbines and Power*, Vol. 133, No. 12, doi: 10.1115/1.4004114, 2011.
- [13] Gravdahl, J. T., Egeland, O.: *Compressor Surge and Rotating Stall, Modelling and Control*, London, ISBN: 978-1-4471-0827-6, 1999.
- [14] Morini, M., Pinelli, M., and Venturini, M.: Application of a One-Dimensional Modular Dynamic Model for Compressor Surge Avoidance, *ASME Turbo Expo 2007: Power for Land, Sea, and Air*, vol. 4, Conference Sponsors: International Gas Turbine Institute, Montreal, Canada, ISBN: 0-7918-4793-4, doi: 10.1115/GT2007-27041, pp. 1425-1434, 2007.
- [15] Link C. Jaw., William T. Cousins., Dong N. WU., and David J. Bryg: Design and Test of a Semi-Passive Flow Control Device for Inlet Distortion Suppression., *Journal of Turbomachinery*, Vol. 123, No. 1, doi: 10.1115/1.1333091, pp. 9-13, 2001.
- [16] Japikse, D.: *Centrifugal Compressor Design and Performance*, Printed in the by Thomson-Shore ed., United states of America: Concepts ETI, ISBN: 978-0933283039, 1996.
- [17] Wiley: *The Jet Engine*, Fifth edition ed., New York: Published in Rolls-Royce, ISBN: 978-1-119-06599-9, August 2015.
- [18] Sánta, I.: "Tervezési Segédlet - Gázturbinás Repülőgép Hajtóművek, BME Vasúti Járművek, Repülőgépek és Hajók Tanszék" (Guide Line for Aircraft Engines Design at BME University), Budapest, 2008.
- [19] Pallag, N.: *A TKT-1 Gázturbinás Sugárhajtómű Áramlástanai Vizsgálata*, Budapest University of Technology and Economics, Department of Aeronautics, Naval Architecture and Railway Vehicles (Master thesis at BME University), Budapest, 2013.
- [20] (online), url: http://www.bridgesofbudapest.com/bridge/chain_bridge (24.06.2017.)
- [21] (online), url: https://en.wikipedia.org/wiki/Airbus_A380 (24.06.2017.)
- [22] (online), url: https://en.wikipedia.org/wiki/General_Electric_GE90 (24.06.2017.)
- [23] (online), url: <http://media.daimler.com/marsMediaSite/en/instance/ko/Mercedes-Benz-Actros.xhtml?oid=9904742> (24.06.2017)

[24] (online), url: <http://behindthewheel.com.au/next-gen-mercedes-benz-actros-launched-australia/2017-mercedes-benz-actros/> (24.06.2017)

[25] (online), url: <https://en.wikipedia.org/wiki/IPhones/> (24.06.2017)

KUTATÁSI CÉLÚ SUGÁRHAJTÓMŰ AERODINAMIKAI ÚJRATERVEZÉSE ÉS VIZSGÁLATA - GÁZ-TURBINA RÉSZEGYSÉGEK VIRTUÁLIS PROTOTÍPUS GYÁRTÁSA

Napjainkban a gáz turbinás hajtóművek jelentik az egyetlen megoldást a nagysebességű kereskedelmi és a katonai repülésben a tolóerő létrehozására, miközben alkalmazásuk széles körben elterjedt az ipar más területein is. A jelen kutatási projekt keretében egy kb. 330 N tolóerő előállítására alkalmas gázturbinás hajtómű akadémiai célú sugárhajtóművé történő aerodinamikai újratervezési lépéseit, az elkészített modell analízisét és az eredmények validálását mutatjuk be. A sugárhajtómű egy egyfokozatú 2.5:1 torlóponthoz tartozó nyomásviszonyú és 43000 fordulat/perces fordulatszámú centrifugálkompresszorral, egyirányú gyűrűs égéstérrel és kb. 1000 K belépő hőmérséklettel rendelkező egyfokozatú turbinából áll. Az aerodinamikai tervezést követően a 3D-s alkatrész modellek és áramlási terek előállítására került sor. Végül a numerikus áramlástan és termikus szimulációk elkészítését követően az eredményt hasonlítottuk össze a tervezés során meghatározott feltételekkel, a rendelkezésre álló mérési eredményekkel validáció céljából, illetve vontunk le következtetéseket a tervezés és az analízis alkalmazhatóságával, pontosságával és hatékonyságával kapcsolatban.

Kulcsszavak: kis-gázturbina, sugárhajtómű, hajtóműtervezés, CAD modell-készítés, CFD, validáció

Zare Foroozan
PhD hallgató
Budapest Műszaki és Gazdaságtudományi Egyetem
Közlekedésmérnöki és Járműmérnöki Kar

Vasúti Járművek, Repülőgépek és Hajók Tanszék

fzare@vrht.bme.hu
orcid.org/0000-0002-5486-5881

Dr. Veress Árpád
egyetemi docens
Budapest Műszaki és Gazdaságtudományi Egyetem
Közlekedésmérnöki és Járműmérnöki Kar

Vasúti Járművek, Repülőgépek és Hajók Tanszék

averess@vrht.bme.hu
orcid.org/0000-0002-1983-2494

Zare Foroozan
PhD Student
Budapest University of Technology and Economics
Faculty of Transporting Engineering and Vehicle
Engineering

Department of Aeronautical, Naval Architecture and
Railway Vehicles

fzare@vrht.bme.hu
orcid.org/0000-0002-5486-5881

Dr. Veress Árpád
Associate Professor
Budapest University of Technology and Economics
Faculty of Transporting Engineering and Vehicle
Engineering

Department of Aeronautical, Naval Architecture and
Railway Vehicles

averess@vrht.bme.hu
orcid.org/0000-0002-1983-2494



http://www.repulestudomany.hu/folyoirat/2017_2/2017-2-22-0390_Foroozan_Zare_Arpád_Veress.pdf